

SCIENTIFIC REPORTS



OPEN

Turing instabilities on Cartesian product networks

Malbor Asllani¹, Daniel M. Busiello², Timoteo Carletti³, Duccio Fanelli⁴ & Gwendoline Planchon^{2,4}

Received: 26 January 2015

Accepted: 10 July 2015

Published: 06 August 2015

The problem of Turing instabilities for a reaction-diffusion system defined on a complex Cartesian product network is considered. To this end we operate in the linear regime and expand the time dependent perturbation on a basis formed by the tensor product of the eigenvectors of the discrete Laplacian operators, associated to each of the individual networks that build the Cartesian product. The dispersion relation which controls the onset of the instability depends on a set of discrete wavelengths, the eigenvalues of the aforementioned Laplacians. Patterns can develop on the Cartesian network, if they are supported on at least one of its constitutive sub-graphs. Multiplex networks are also obtained under specific prescriptions. In this case, the criteria for the instability reduce to compact explicit formulae. Numerical simulations carried out for the Mimura-Murray reaction kinetics confirm the adequacy of the proposed theory.

Patterns are widespread in nature and appear in large plethora of different conformations. From chemistry to biology, passing through physics, beautiful spatially extended motifs are found which spontaneously emerge from an ensemble made of interacting microscopic actors. The spirals in chemical reactions, the colorful patterns on fish skin, and the maculated fur coat of felines are all examples which testify on the intrinsic ability of natural system to self-organize, both in space and in time^{1,2}.

The proto-typical approach to patterns formation in reaction-diffusion processes dates back to Alan Turing's seminal paper on morphogenesis³. Working within a simplified deterministic model for two species in mutual interactions, Turing proved that a homogeneous fixed point can turn unstable to external perturbations. A symmetry breaking instability can in fact develop which is seeded by diffusion and necessitates of an activator-inhibitor scheme of interaction between factors. When the conditions for the Turing instability are satisfied, the perturbation grows exponentially at short times and the system evolves towards an asymptotic stationary stable attractor, characterized by a spatially inhomogeneous density distribution. Mathematical conditions for the onset of the instability can be obtained via a linear stability analysis, which requires expanding the imposed perturbation on the complete basis formed by the eigenvectors of the Laplacian operators on the chosen domain. Turing instabilities are usually studied on regular lattices or continuous supports. The theory of patterns formation extends however to reaction-diffusion systems defined on a complex graph, as illustrated in the pioneering paper by Othmer and Scriven⁴, and recently revisited by Nakao and Mikhailov⁵. In this case the domain of the dispersion relation, from which the instability conditions ultimately descend, is the spectrum of the discrete Laplacian associated to the embedding network. Laplacian eigenvalues determine in fact the spatial characteristics of the emerging patterns, when the system is defined on a heterogeneous complex support. Turing patterns for systems defined on a complex graph materialize in a segregation into activator-rich and activator-poor nodes⁷. As discussed in⁶, self-organized patterns can also manifest on multiplex, networks of networks assembled as adjacent layers⁸⁻¹⁵. Remarkably, patterns on a multiplex

¹Dipartimento di Scienza e Alta Tecnologia, University of Insubria, via Valleggio 11, 22100 Como, Italy. ²Department of Physics and Astronomy G. Galilei, University of Padova, via Marzolo 8, 35131 Padova, Italy. ³Department of mathematics and Namur Center for Complex Systems - naXys, University of Namur, rempart de la Vierge 8, B 5000 Namur, Belgium. ⁴Dipartimento di Fisica e Astronomia, University of Florence and INFN, Via Sansone 1, 50019 Sesto Fiorentino, Florence, Italy. Correspondence and requests for materials should be addressed to T.C. (email: timoteo.carletti@unamur.be)

can be instigated by a constructive interference between layers, also when the Turing-like instability is prevented to occur on each single layer taken separately. In other cases, inter-layer diffusion can instead act a destructive pressure on the process of pattern formation⁶.

Building on these premises, we here aim at applying the theory of Turing instability for reaction diffusion systems defined on Cartesian networks. These latter are assembled as the Cartesian product of simpler networks, the fundamental building blocks in the process of hierarchical aggregation. Regular grids, cubes, and their counterparts in higher dimensions are for instance obtained from the Cartesian product of linear chains. Besides the interest from a graph theory point of view^{16,19}, Cartesian product (also referred to as Cartesian networks in the following) have been recently used in the framework of control processes¹⁷ and systems synchronization¹⁸.

In this paper we shall adapt the linear instability analysis to the relevant setting of the Cartesian networks, and elaborate on the condition for the instability, by expanding the perturbation on a generalized basis formed by the tensor product of the eigenvectors of the discrete Laplacian operators, defined on each individual network. For a sake of clarity we will illustrate the theory with reference to the simplified setting where the Cartesian product involves two distinct networks. Clearly, one can straightforwardly extend the theory to Cartesian products made by more than two networks. It is worth emphasizing that a Cartesian network can be equivalently treated as a standard network, specified by a global adjacency matrix and notwithstanding its parcelization in elementary sub-components. Hence, the conditions for the emergence of self-organized patterns in a reaction diffusion system defined on a Cartesian support could be effectively addressed by following the general strategy outlined in⁵. However, by taking advantage of the peculiar structure of Cartesian networks, one can gain insight into the onset of the instability by tracing it back to the properties of the underlying simplex networks. This level of understanding cannot be achieved when carrying out a direct diagonalization of the global Laplacian matrix associated to the Cartesian product network. To shed light on these aspects, the process of patterns formation on the Cartesian support will be thoroughly discussed in conjunction with the standard analysis which applies to each of the graphs taken independently.

As an interesting application, we will then consider the special case of multiplex networks that can be factorized as Cartesian products of smaller basic networks and prove that the patterns can be created or destroyed by adding more layers to the structure. On a wider perspective, this result applies to reaction-diffusion systems defined on a generic network, which can be factorized as the Cartesian product of smaller networks. The conditions for the instability of the scrutinized system can be hence reformulated in terms of the smaller, hence more tractable, factor networks.

The paper is organized as follows. In the next Section we will present the general theory of Cartesian product networks and formulate the problem of patterns formation for reaction—diffusion systems defined on such networks. For a generic choice of the diffusivities, we shall prove that patterns emerge in the Cartesian product provided they can develop in at least one of the two networks from which the Cartesian support originates. In this respect, Cartesian products are more prone to exhibit Turing instabilities than their corresponding factor networks. In the limiting case when the diffusivities do not depend on the topology of the networks, but just on the species ability to relocate to neighbors sites, Turing patterns can set in if and only if the instability takes place on both factor networks. Our analytical conclusions will be challenged numerically by employing the Mimura—Murray model²² as a representative reaction scheme. We will then turn to investigate the conditions for the emergence of self-organized patterns on degenerate multiplex networks - the same network is repeated on all layers - an important case study which can be handled as an immediate byproduct of our analysis. Finally, in the last Section, we will sum up and conclude.

Results

Given two networks G and H , being respectively characterized by n_G and n_H nodes, hereby denoted $g_i \in V_G$ and $h_j \in V_H$, and by edges $(g_i, g_j) \in E_G$ and $(h_i, h_j) \in E_H$, one can build^{16,19} their *Cartesian product* $G \square H$, that is the network composed by $n_G n_H$ nodes $V_G \times V_H$ and whose edges $E_{G \square H}$ are defined by:

$$e = ((g_1, h_1), (g_2, h_2)) \in E_{G \square H} \text{ iff } g_1 = g_2 \text{ and } (h_1, h_2) \in E_H \text{ or } h_1 = h_2 \text{ and } (g_1, g_2) \in E_G. \quad (1)$$

We represent in Fig. 1 an example of a Cartesian product network built from two Watts-Strogatz networks²³.

Let A^G , respectively A^H , be the adjacency matrix of the network G , respectively H . Then the adjacency matrix of the Cartesian product network $G \square H$ is given by

$$A^{G \square H} = A^G \otimes \mathbb{I}_{n_H} + \mathbb{I}_{n_G} \otimes A^H, \quad (2)$$

where \mathbb{I}_n is the $n \times n$ identity matrix and \otimes is the Kronecker product. Let us recall that the Kronecker product of two matrices A and B , is the matrix

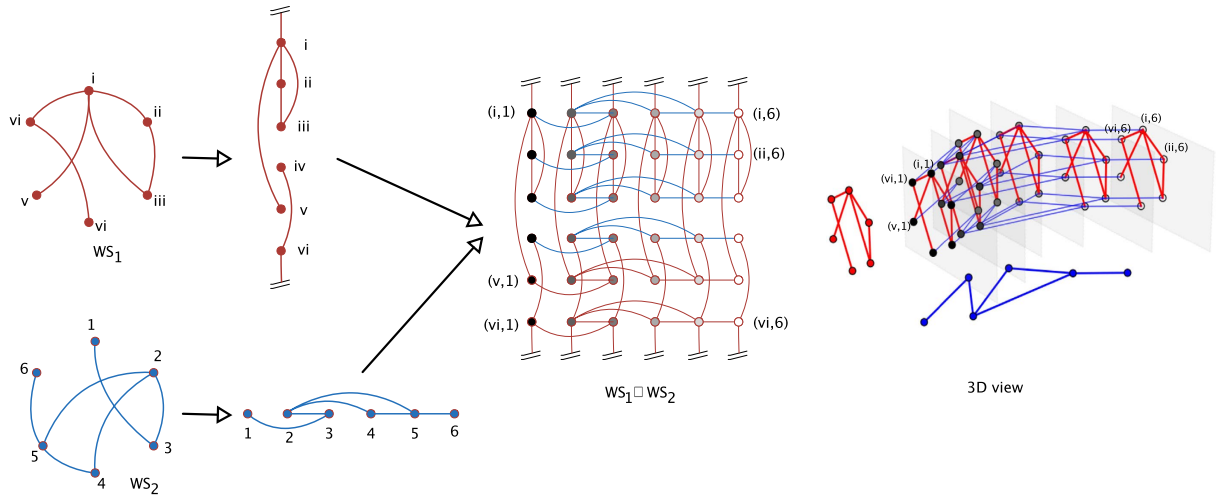


Figure 1. The Cartesian product of two Watts-Strogatz²³ 1D networks. Left panel: the two Watts-Strogatz networks WS_1 (red on line) and WS_2 (blue on line) are presented by using respectively a circular and a linear layout. This latter yields the planar representation of the Cartesian Product network, as displayed in the middle panel. According to this picture the Cartesian network appears as a perturbation of a regular 2D lattice. Right panel: the 3D view of the Cartesian Product. Links in the Cartesian Product are colored as in the individual factor network (the same convention has been used in the middle panel). Nodes are instead colored according to a grey scale for each layer of the product, from white (corresponding to node 6 in WS_2) to black (corresponding to node 1 in WS_2). The cylindrical shape is obtained by imposing a circular layout to WS_1 and a chain layout to WS_2 .

$$A \otimes B = \begin{pmatrix} a_{11}B & \dots & a_{1n}B \\ \vdots & \ddots & \vdots \\ a_{n1}B & \dots & a_{nn}B \end{pmatrix},$$

where a_{ij} are the elements of matrix A . Let $L^G = A^G - D^G$ (respectively $L^H = A^H - D^H$) be the Laplacian matrix of the network G (respectively of H), where D^G is the diagonal matrix whose entries are the degrees of the network G (similarly for D^H). Then the Laplacian matrix of the Cartesian product network $G \square H$ reads:

$$L^{G \square H} = L^G \otimes \mathbb{I}_{n_H} + \mathbb{I}_{n_G} \otimes L^H. \tag{3}$$

From the latter equation, it straightforwardly follows that the eigenvalues of $L^{G \square H}$ are of the form

$$\Lambda_{\alpha\beta}^{G \square H} = \Lambda_{\alpha}^G + \Lambda_{\beta}^H \quad \forall \alpha = 1, \dots, n_G \text{ and } \beta = 1, \dots, n_H, \tag{4}$$

that is the eigenvalues of the Laplacian matrix associated to the Cartesian product are obtained as the sum of the eigenvalues of the Laplacian operators of each factor networks. Moreover, the eigenvectors of $L^{G \square H}$ are given by $\phi_{\alpha\beta} = (\phi_{\alpha}^G, \phi_{\beta}^H)$, where ϕ_{α}^G and ϕ_{α}^H stand for the eigenvectors of respectively L^G and L^H . In fact:

$$\begin{aligned} L^{G \square H} (\phi_{\alpha}^G, \phi_{\beta}^H) &= (L^G \otimes \mathbb{I}_{n_H}) (\phi_{\alpha}^G, \phi_{\beta}^H) + (\mathbb{I}_{n_G} \otimes L^H) (\phi_{\alpha}^G, \phi_{\beta}^H) \\ &= (L^G \phi_{\alpha}^G, \phi_{\beta}^H) + (\phi_{\alpha}^G, L^H \phi_{\beta}^H) = (\Lambda_{\alpha}^G \phi_{\alpha}^G, \phi_{\beta}^H) + (\phi_{\alpha}^G, \Lambda_{\beta}^H \phi_{\beta}^H) \\ &= \Lambda_{\alpha}^G (\phi_{\alpha}^G, \phi_{\beta}^H) + \Lambda_{\beta}^H (\phi_{\alpha}^G, \phi_{\beta}^H) = (\Lambda_{\alpha}^G + \Lambda_{\beta}^H) (\phi_{\alpha}^G, \phi_{\beta}^H). \end{aligned}$$

Let us observe that L^G and L^H are zero sum symmetric and negative—semidefinite matrices and so it is $L^{G \square H}$. Hence, the eigenvalues $\Lambda_{\alpha\beta}^{G \square H}$ are all negative, except for the largest one which is identical to zero. We will organize the list eigenvalues so that the first position ($\alpha = \beta = 1$) reads always zero, the largest eigenvalue. Hence, $\Lambda_1^{G \square H} = 0$.

Reaction-Diffusion systems on Cartesian product networks. Let us now consider a reaction—diffusion system defined on a Cartesian product network $G \square H$. To this end we introduce two species whose continuous densities are labelled u and v . The two species undergo local interaction when they

share one of the $n_G n_H$ nodes of $G \square H$ and diffuse among adjacent sites via existing links. Denote with $D_u^G \geq 0$, respectively $D_v^G \geq 0$, the diffusion coefficient of species u , respectively v , on network G . For network H , one can introduce the homologous quantities $D_u^H \geq 0$ and $D_v^H \geq 0$. In the following we shall indicate with u_{gh} and v_{gh} the concentrations of respectively u and v at node $(gh) \in G \square H$. As usual, local rules of interaction among species translate in non linear functions of the concentration amount, hereafter $f(u_{gh}, v_{gh})$ and $g(u_{gh}, v_{gh})$. The diffusion is in turn modeled by resorting to conventional Laplacian operators. In formulae:

$$\begin{cases} \dot{u}_{gh} = f(u_{gh}, v_{gh}) + \mathcal{L}_u u_{gh} \\ \dot{v}_{gh} = g(u_{gh}, v_{gh}) + \mathcal{L}_v v_{gh} \end{cases} \quad \forall g \in \{1, \dots, n_G\}, h \in \{1, \dots, n_H\} \text{ and } t > 0. \tag{5}$$

where the diffusion operator \mathcal{L}_s (with $s = u, v$) reads:

$$\mathcal{L}_s = D_s^G L^G \otimes \mathbb{I}_{n_H} + D_s^H \mathbb{I}_{n_G} \otimes L^H \quad \text{for } s = u, v. \tag{6}$$

Notice that u_{gh} can be written as (u_g^G, u_h^H) , and hence $(L^G \otimes \mathbb{I}_{n_H})(u_g^G, u_h^H) = (L^G u_g^G, u_h^H)$. On the other hand, $L^G u_g^G = \sum_{g'} L_{gg'}^G u_{g'}^G$, which implies $(L^G u_g^G, u_h^H) = (\sum_{g'} L_{gg'}^G u_{g'}^G, u_h^H) = \sum_{g'} L_{gg'}^G u_{g'h}$. Similar considerations hold for $\mathbb{I}_{n_G} \otimes L^H$, and one can therefore rewrite (5) as:

$$\begin{cases} \dot{u}_{gh} = f(u_{gh}, v_{gh}) + D_u^G (L^G u)_{gh} + D_u^H (L^H u)_{gh} \\ \quad = f(u_{gh}, v_{gh}) + D_u^G \sum_{g'} L_{gg'}^G u_{g'h} + D_u^H \sum_{h'} L_{h'h}^H u_{gh'} \\ \dot{v}_{gh} = g(u_{gh}, v_{gh}) + D_v^G (L^G v)_{gh} + D_v^H (L^H v)_{gh} \\ \quad = g(u_{gh}, v_{gh}) + D_v^G \sum_{g'} L_{gg'}^G v_{g'h} + D_v^H \sum_{h'} L_{h'h}^H v_{gh'} \end{cases} \tag{7}$$

To progress in the analysis we shall assume that an homogeneous solution of the above equations exists, i.e. $(u_{gh}, v_{gh}) = (\hat{u}, \hat{v})$, for all g and h such that $f(\hat{u}, \hat{v}) = g(\hat{u}, \hat{v}) = 0$. In addition, we will require the homogeneous fixed point (\hat{u}, \hat{v}) to be stable, which in turn amounts to impose $\text{tr}(J) = \partial_u f + \partial_v g < 0$ and $\det(J) = \partial_u f \partial_v g - \partial_v f \partial_u g > 0$, where J stands for the Jacobian matrix evaluated at (\hat{u}, \hat{v}) (to keep the notation simple and because f and g do not depend on the nodes index, we have replaced u_{gh} and v_{gh} by u and v in the former and in their derivatives). Following the standard Turing recipe, we set down to study the conditions that yield an exponential growth of a non-homogeneous perturbation around (\hat{u}, \hat{v}) . We hence define $\delta u_{gh} = u_{gh} - \hat{u}$ and $\delta v_{gh} = v_{gh} - \hat{v}$ and linearize system (7) around the equilibrium

$$\begin{cases} \dot{\delta u}_{gh} = f_u \delta u_{gh} + f_v \delta v_{gh} + D_u^G \sum_{g'} L_{gg'}^G \delta u_{g'h} + D_u^H \sum_{h'} L_{h'h}^H \delta u_{gh'} \\ \dot{\delta v}_{gh} = g_u \delta u_{gh} + g_v \delta v_{gh} + D_v^G \sum_{g'} L_{gg'}^G \delta v_{g'h} + D_v^H \sum_{h'} L_{h'h}^H \delta v_{gh'} \end{cases} \tag{8}$$

where f_u, f_v, g_u and g_v are the derivatives of f and g with respect to u and v evaluated at the equilibrium point (\hat{u}, \hat{v}) .

To go one step further we expand δu_{gh} and δv_{gh} on the eigenbasis of the Laplacian matrix for $G \square H$ and look for solution of system (8) in the form:

$$\delta u_{gh} = \sum_{\alpha\beta} U_{\alpha\beta} \phi_{\alpha\beta}^{gh} e^{\lambda_{\alpha\beta} t} \quad \text{and} \quad \delta v_{gh} = \sum_{\alpha\beta} V_{\alpha\beta} \phi_{\alpha\beta}^{gh} e^{\lambda_{\alpha\beta} t}.$$

By inserting the previous relations into the linearized system (8), one readily finds that the following condition should be met for a non-trivial solution to exist:

$$\det(\tilde{J} - \lambda_{\alpha\beta} \mathbb{I}) = 0,$$

where

$$\tilde{J} = \begin{pmatrix} f_u + D_u^G \Lambda_\alpha^G + D_u^H \Lambda_\beta^H & f_v \\ g_u & g_v + D_v^G \Lambda_\alpha^G + D_v^H \Lambda_\beta^H \end{pmatrix},$$

that is

$$\lambda_{\alpha,\beta}^2 - P(\Lambda_\alpha^G, \Lambda_\beta^H) \lambda_{\alpha,\beta} + Q(\Lambda_\alpha^G, \Lambda_\beta^H) = 0, \tag{9}$$

where $P(\Lambda_\alpha^G, \Lambda_\beta^H)$ and $Q(\Lambda_\alpha^G, \Lambda_\beta^H)$ are defined as:

$$\begin{aligned}
 P(\Lambda_\alpha^G, \Lambda_\beta^H) &= \text{tr}(J) + \Lambda_\beta^H(D_u^H + D_v^H) + \Lambda_\alpha^G(D_u^G + D_v^G) \\
 Q(\Lambda_\alpha^G, \Lambda_\beta^H) &= \det(J) + \Lambda_\beta^H(D_u^H g_v + D_v^H f_u) + \Lambda_\alpha^G(D_u^G g_v + D_v^G f_u) \\
 &\quad + (\Lambda_\beta^H)^2 D_u^H D_v^H + \Lambda_\beta^H \Lambda_\alpha^G (D_u^H D_v^G + D_u^G D_v^H) + (\Lambda_\alpha^G)^2 D_u^G D_v^G.
 \end{aligned}
 \tag{10}$$

Let us observe that P is always negative because of the stability assumption ($\text{tr}(J) < 0$) and since $\Lambda_\beta^H \leq 0$ and $\Lambda_\alpha^G \leq 0$. The exponential instability manifests provided the real part of $\lambda_{\alpha\beta}$ gets positive over a bounded portion of the plane $(\Lambda_\beta^H, \Lambda_\alpha^G)$. For this reason, we shall solely concentrate on the largest root of equation (9):

$$\lambda^{G \square H}(\Lambda_\alpha^G, \Lambda_\beta^H) = \frac{P(\Lambda_\alpha^G, \Lambda_\beta^H) + \sqrt{P^2(\Lambda_\alpha^G, \Lambda_\beta^H) - 4Q(\Lambda_\alpha^G, \Lambda_\beta^H)}}{2}.$$

whose real part is also called the dispersion relation. Turing instability develops on the Cartesian network provided

$$Q(\Lambda_\alpha^G, \Lambda_\beta^H) < 0. \tag{11}$$

within a finite domain in Λ_β^H and Λ_α^G . In the following we shall set $\lambda^{G \square H}(\Lambda_\alpha^G, \Lambda_\beta^H) \equiv \lambda_{\alpha,\beta}(\Lambda_\alpha^G, \Lambda_\beta^H)$ and $Q^{G \square H}(\Lambda_\alpha^G, \Lambda_\beta^H) \equiv Q(\Lambda_\alpha^G, \Lambda_\beta^H)$ to make explicit reference to the embedding Cartesian topology.

The above derivation can be formally adapted to the simpler case where the reaction-diffusion system is defined on a standard graph G . In this case the condition for the existence of Turing patterns amounts to imposing $Q^G(\Lambda_\alpha^G) = \det(J) + \Lambda_\alpha^G(D_u^G g_v + D_v^G f_u) + (\Lambda_\alpha^G)^2 D_u^G D_v^G < 0$, inside a bounded interval of Λ_α^G . Importantly, $Q^G(\Lambda_\alpha^G) = Q^{G \square H}(\Lambda_\alpha^G, 0)$. Similar considerations hold for graph H , which is combined to G to yield the Cartesian network $G \square H$. In practical terms, the dispersion relation which controls the instability on a Cartesian support is a multi-dimensional function (two dimensional, for the case under exam), which reduces to the conventional one dimensional function, when projected on each of the independent subspaces that compose the Cartesian backing. Notice that the above conclusions can be also reached by employing a straightforward two dimensional extension of the network-targeted Fourier transform introduced in^{20,21} to the current multi-dimensional setting.

Starting from this scenario, it is interesting to elaborate on the mathematical conditions that underly the emergence of collective patterns on a Cartesian support, in relation to the mechanisms which seed the homologous instabilities on the composing graphs, taken separately. Are Cartesian patterns reminiscent of the instability that occur on each layer of the assembly? To answer this question it is entirely devoted the remaining part of the paper.

Different diffusion constants on distinct graphs. Let us start by considering the general case where the diffusion coefficients for each species are assumed to depend on the hosting network, namely $D_u^G \neq D_u^H$ and $D_v^G \neq D_v^H$. Imagine that Turing patterns can develop when the inspected reaction-diffusion system is hosted on G . Then, as we shall prove hereafter, the patterns can invade the Cartesian support $G \square H$. Similar conclusions obviously hold when the dual scenario is considered, i.e. when the patterns are allowed to develop on graph H , instead of G .

Since Turing patterns can be found by hypothesis on network G , there exists at least one $\hat{\alpha} \in \{1, \dots, n_G\}$ such that $Q^G(\Lambda_{\hat{\alpha}}^G) < 0$. Consider the eigenvalue $\Lambda_{\hat{\alpha}1}^{G \square H} = \Lambda_{\hat{\alpha}}^G + \Lambda_1^H = \Lambda_{\hat{\alpha}}^G$ (where in the last step we made use of $\Lambda_1^H = 0$) and write the following chain of relations:

$$Q^{G \square H}(\Lambda_{\hat{\alpha}}^G, \Lambda_1^H) \equiv Q^{G \square H}(\Lambda_{\hat{\alpha}}^G, 0) = Q^G(\Lambda_{\hat{\alpha}}^G) < 0.$$

The same modes which are unstable on G , are also destabilized when the reaction-diffusion system is made to evolve on the Cartesian support $G \square H$. The network $G \square H$ can hence exhibit Turing patterns, the perturbation being localized on a set of unstable modes which includes (or coincides with) those active on G . If the spectrum of the Laplacian was continuum, one could always delimit, by continuity of $Q^{G \square H}$, a finite portion of the parameter plan (Λ^G, Λ^H) , adjacent to the degenerate line $(\Lambda^G, 0)$, for which $Q^{G \square H} < 0$. However, the spectrum of the Laplacian operator is discrete. One should therefore require a sufficiently small $|\Lambda_\beta^H|$ to exist, so that $Q^{G \square H}(\Lambda_{\hat{\alpha}}^G, \Lambda_\beta^H) < 0$, for non trivial modes of the Cartesian support could be triggered unstable.

To make this concept more explicit, we consider the celebrated Mimura-Murray model²², which we shall assume to specify the reaction terms. More specifically we will set $f(u, v) = ((a + bu - u^2)/c - v)u$ and $g(u, v) = (u - (1 + dv))v$, where a, b, c and d are constant parameters. The Mimura-Murray model possesses six equilibria, whose stability depends on the value of the above parameters. We will hereby set $a = 35, b = 16, c = 9$ and $d = 0.4$ and focus on the homogeneous stationary solution $\hat{u} = 1 + (bd - 2d - c + \sqrt{\Delta})/(2d), \hat{v} = (bd - 2d - c + \sqrt{\Delta})/(2d^2)$ where $\Delta = (bd - 2d - c)^2 + 4d^2$

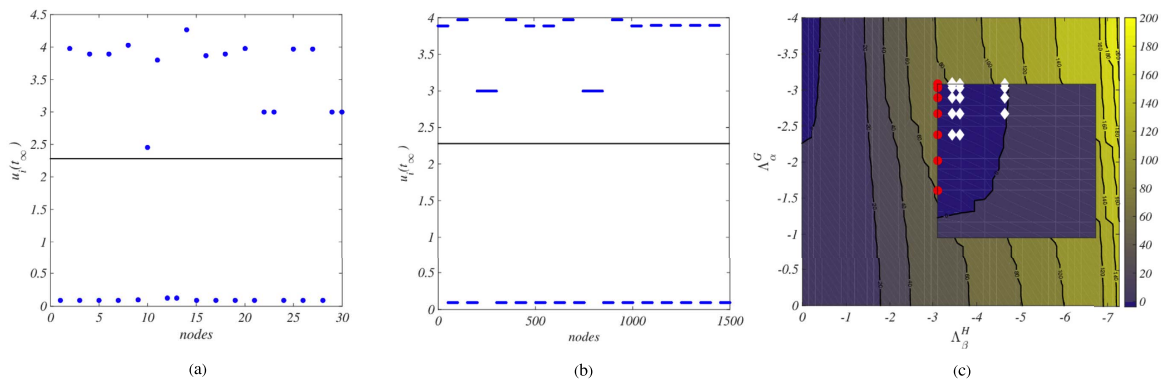


Figure 2. Turing patterns for the Mimura-Murray model on the Cartesian product $G \square H$. Panel (a): G exhibits Turing patterns, the asymptotic concentration of species u (circles, blue online) varies from node to node and differs from the corresponding equilibrium value $\hat{u} \sim 2.28$ (horizontal line). The diffusion constants are set so that Turing patterns cannot develop on graph H (data not shown). Panel (b): the Mimura-Murray model defined on the cartesian product $G \square H$ displays Turing patterns. Once again the asymptotic concentration of species u (circles, blue online) varies from node to node and differs from the predicted equilibrium solution (horizontal black line). Panel (c): level sets of the function $Q_{\alpha\beta}^{G \square H}$. Notice the (dark blue online) zone in the top left corner of the figure (enlarged in the inset) where the function takes negative values. The ensemble of vertical (red online) circles represents the eigenvalues of L^G . As anticipated, $Q^{G \square H}(\Lambda_\alpha^G, 0) = Q^G(\Lambda_\alpha^G) < 0$, which points to the existence of Turing instability on subspace G . White diamonds identify the pairs $(\Lambda_\alpha^G, \Lambda_\beta^H)$ for which $Q^{G \square H}(\Lambda_\alpha^G, \Lambda_\beta^H) < 0$: patterns are hence supported on the Cartesian product network $G \square H$. On the other hand, for $\Lambda_\alpha^G = 0$, the function $Q^{G \square H}$ is positive. One cannot find Λ_β^H for which $Q^{G \square H}(0, \Lambda_\beta^H) < 0$, in agreement with our initial working assumption: patterns cannot grow on graph H , when taken isolated. Here, G and H are Watts-Strogatz²³ networks composed respectively of $n_G = 30$ and $n_H = 50$ nodes. Their associated links rewiring probabilities are taken to $p_G = 0.01$ and $p_H = 0.04$ and the average degree are given by $\langle k_G \rangle = 2$ and $\langle k_H \rangle = 4$. The diffusion coefficients are set to the values $D_u^G = 0.01$, $D_v^G = 2.1$, $D_u^H = 1.12$ and $D_v^H = 2.6$. The initial condition is a perturbation of the homogeneous fixed point (\hat{u}, \hat{v}) . Such externally imposed perturbation is node dependent, hence inhomogeneous, drawn from a uniform distribution and scaled with an amplitude factor $\delta = 0.005$.

$(a + b - 1)$. It is immediate to realize that $\det(J) > 0$ and $\text{tr}(J) < 0$, hence the selected fixed point is stable. The diffusion coefficients are assigned as discussed in the caption of Fig. 2. In particular, patterns can develop when the Mimura-Murray system is let evolve on graph G . At variance, Turing instability cannot take place on graph H . When the system is instead hosted on the Cartesian support $G \square H$, as obtained by composing together the individual graphs G and H , patterns can materialize, as demonstrated in Fig. 2. The generalized dispersion relation takes indeed positive values over a finite portion of the discrete two dimensional support $(\Lambda_\alpha^G, \Lambda_\beta^H)$ as it can be appreciated by visual inspection of panel c of Fig. 2.

The diffusion is the same on distinct networks. Consider now the simpler setting where the diffusion coefficients are assumed identical on all graphs composing the Cartesian networks. In formulae we require $D_u^G = D_u^H = D_u$ and $D_v^G = D_v^H = D_v$. Also the kinetics parameters do not depend on the reaction site. Under this working hypothesis, Turing patterns are allowed on the Cartesian network $G \square H$, if and only if they can also develop on both G and H . To prove our claim, we remark that the assumption of identical diffusivities enables one to simplify the dispersion relation and Eqs. (10) and, in particular, we get:

$$Q(\Lambda_\alpha^G, \Lambda_\beta^H) = \det(J) + (\Lambda_\alpha^G + \Lambda_\beta^H)(D_u g_v + D_v f_u) + D_u D_v (\Lambda_\beta^H + \Lambda_\alpha^G)^2.$$

Hence, the instability takes place on the Cartesian support if $D_u g_v + D_v f_u > 0$ and $(D_u g_v + D_v f_u)^2 - 4 \det(J) D_u D_v > 0$. On the other hand, when these latter inequalities are matched, Turing patterns develop on both G and H , provided their discrete Laplacian eigenvalues populate the interval where the dispersion relations for each single graph, λ_α^G and λ_α^H , are positive.

Degenerate multiplex as the Cartesian product of two graphs. Assume G to be an open one dimensional chain, with nearest neighbors connections. This configuration is also termed *path* in the literature, and differs from a ring or cycle, because it lacks periodic boundary conditions. Then, for any arbitrary choice of network H , the cartesian product $G \square H$ is a multiplex with peculiar characteristics.

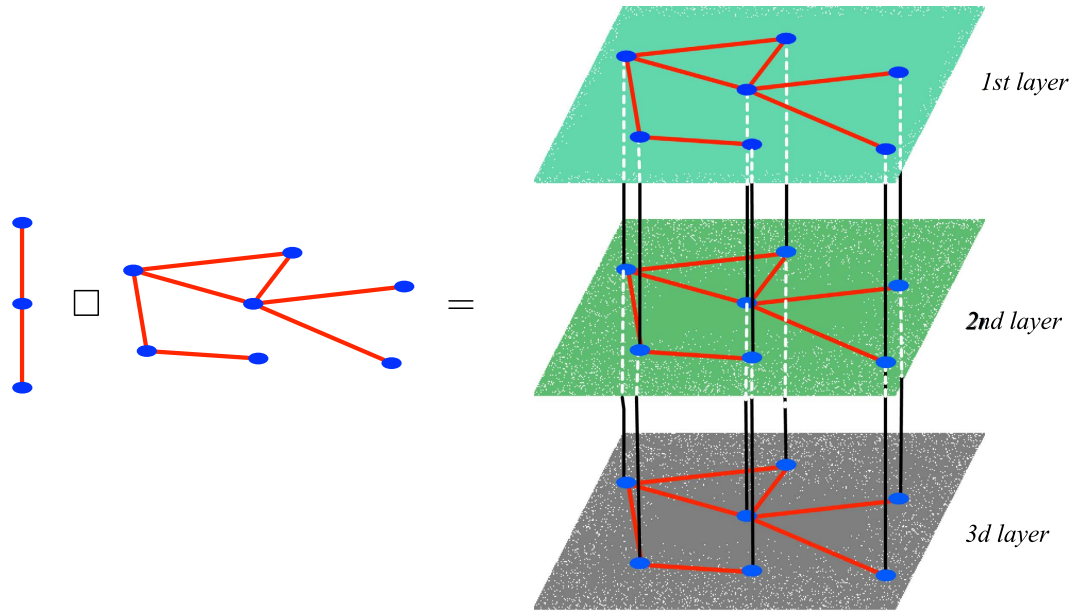


Figure 3. The degenerate multiplex. The Cartesian product of $G = \bullet - \bullet - \bullet$ and a generic graph H .

On each layer of the multiplex the same network H is repeated. Inter-layer connections are established only between adjacent layers, as depicted in Fig. 3.

If we are interested in investigating the possibility of a Turing like instability for a generic reaction-diffusion system defined on such a multiplex, one cannot resort to the approach discussed in⁶. The multiplex is in fact degenerate, meaning that the layers are identical by construction and their associated spectra coincide. This clearly implies dealing with repeated eigenvalues a condition which violates the hypothesis on which the analysis of⁶ builds. It is however worth emphasizing that the analysis of⁶ can be extended to the case where the eigenvalues are indeed repeated, at the price of some additional complications in the calculations. Following the above conclusion, we can however expect Turing patterns to materialize on the multiplex support, if the reaction-diffusion system under inspection can undergo a diffusion driven instability when placed on the path network G . As we shall argue in the following, this request translates in a compact condition for the instability to develop on the multiplex support. In fact, the homogenous equilibrium is unstable to external inhomogeneous perturbation, for a reaction diffusion-system evolving on G , provided $f_u D_G^v + g_v D_G^u > 0$ and $(f_u D_G^v + g_v D_G^u)^2 - 4 \det(J) D_G^u D_G^v > 0$. On the other hand, the eigenvalues of the Laplacian operator defined on G can be written in a closed form as:

$$\Lambda_\alpha^G = -2 + 2 \cos \frac{\alpha - 1}{n_G} \pi \quad \alpha \in \{1, \dots, n_G\}. \tag{12}$$

For a given reaction kinetics, Turing patterns can flourish on G , if and only if there exists at least on eigenvalue Λ_α^G for which $Q^G(\Lambda_\alpha^G) < 0$, namely

$$q_- < \Lambda_\alpha^G < q_+, \tag{13}$$

where

$$q_\pm = \frac{-(f_u D_G^v + g_v D_G^u) \pm \sqrt{(f_u D_G^v + g_v D_G^u)^2 - 4 \det(J) D_G^u D_G^v}}{2 D_G^u D_G^v}, \tag{14}$$

are the two positive roots of $Q_\alpha^G = 0$. When condition (13) is met, and by virtue of the analysis carried out above, the patterns can invade the multiplex support. In Fig. 4 we provide a direct evidence of the phenomenon, employing again the Mimura-Murray reaction model as the reference case study. In our results, no correlation between the asymptotic values of u_i (or v_i) and the node degree is observed, at variance with the conclusion of⁵. This is an intriguing difference which deserves to be further investigated, in relation to the system size of the employed networks and their intrinsic topological features.

Another interesting case to consider is when G is the complete graph with n_G nodes, namely a network with all-to-all connections but self-loops. Then, for any network H , the Cartesian product $G \square H$ is a multiplex, which hosts on every layer a replica of H , each node of a given layer being directly

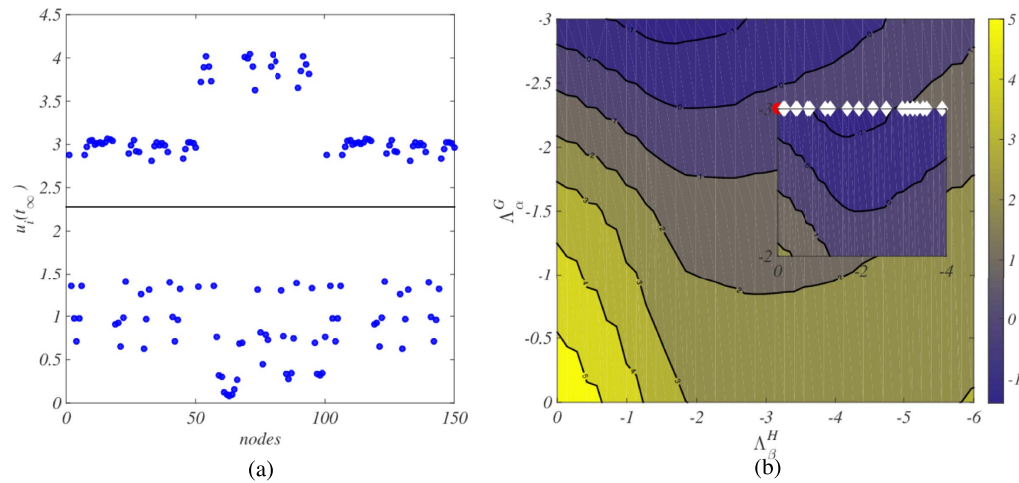


Figure 4. Turing patterns for the Mimura-Murray model on a degenerate multiplex support. The multiplex is built as the Cartesian product $G \square H$. Here, $G = \bullet-\bullet-\bullet$ (namely, it is a linear chain with nearest neighbors connections) and H is a Watts-Strogatz²³ network composed by $n_H = 50$ nodes, with a probability to rewire a link equal to $p_H = 0.04$ and average degree $\langle k_H \rangle = 4$. Panel (a): asymptotic distribution for the concentration of species u (circles, blue online) on each node of the Cartesian product $G \square H$. The recorded concentration varies from node to node and differs from the deputed equilibrium value $\hat{u} \sim 2.28$ (horizontal black line). For the selected parameters (see below), the Mimura-Murray model is Turing unstable on the linear chain G . Turing patterns cannot develop instead, when the reaction-diffusion model is made to evolve on the Watts–Strogatz network H alone. Panel (b): level sets of the function $Q_{\alpha\beta}^{G \square H}$. In the top border of the picture (region enlarged in the inset, dark blue online) the function assumes negative values. The (red online) circle identifies the unstable eigenvalue of the Laplacian operator associated to the linear chain. As anticipated, it falls in the region $Q^{G \square H}(\Lambda_\alpha^G, 0) = Q^G(\Lambda_\alpha^G) < 0$, hence signaling the presence of Turing-like patterns on G . The white diamonds refer to the pairs $(\Lambda_\alpha^G, \Lambda_\beta^H)$ for which $Q^{G \square H}(\Lambda_\alpha^G, \Lambda_\beta^H) < 0$, thus implying the existence of the instability on the Cartesian product $G \square H$. We remark that for $\Lambda_\alpha^G = 0$, the function $Q^{G \square H}$ is positive definite: patterns cannot emerge when the diffusion of the interacting species is confined on graph H . Here, the diffusion coefficients are set to the representative values $D_u^G = 0.005$, $D_v^G = 1.8$, $D_u^H = 0.12$ and $D_v^H = 1.3$. The initial condition is assigned as explained in the caption of Fig. 2.

connected to all its specular *images* on the other layers. The number of nodes of network G determines therefore the number of layers of the Cartesian multiplex. Based on the above, we can readily infer an explicit condition for the existence of Turing instability on the generalized Cartesian support. The only non trivial eigenvalue of the complete graph is $-n_G$ (with multiplicity $n_G - 1$) and condition (13) yields $q_- < -n_G < q_+$. In other words, the number of nodes of G , or equivalently the number of layers in the multiplex, can act as a control parameter to instigate, or alternatively dissolve, the Turing instability. In Fig. 5 we provide a numerical demonstration of the predicted phenomenon. Patterns can be seen on the Cartesian multiplex, for a given choice of H and of the reaction kinetics, only if the number of nodes of the complete graph G falls within a bounded interval. Once again, the asymptotic concentration u_i (or, alternatively, v_i) does not correlate with the degree of the corresponding node i : all the nodes belonging to the same layer in the left panel of Fig. 5 host the same concentration, irrespectively of their associated degree. At variance, nodes with the same degree across layers can display different concentration amount.

Conclusions

Reaction-diffusion systems on complex networks are gaining attention because of their multifaceted applications to a vast realm of interdisciplinary problems. As follows a symmetry breaking instability, seeded by diffusion, a stable homogeneous fixed point of the examined reaction kinetics can turn unstable to inhomogeneous perturbation. This event is the precursor of a Turing pattern, which is eventually approached by the system in its late time evolution. The conditions that underly the spontaneous emergence of self-organized patterns can be obtained via a standard linear stability analysis, which requires expanding the imposed perturbation on a basis formed by the eigenvectors of the network Laplacian operator. Importantly, the associated eigenvalues play the role of non trivial wavelengths for the embedding network support.

Starting from this setting, we have here analyzed the case of Cartesian networks, namely complex support assembled as the Cartesian product of simpler networks, and elaborated on the conditions for the Turing instability to set in. To this aim, we introduced and exploited a generalized basis for tracking the perturbation in its linear regime of evolution. This is the tensor product of the eigenvectors of the discrete Laplacian operators, defined on each individual network. For simplicity we focused from the

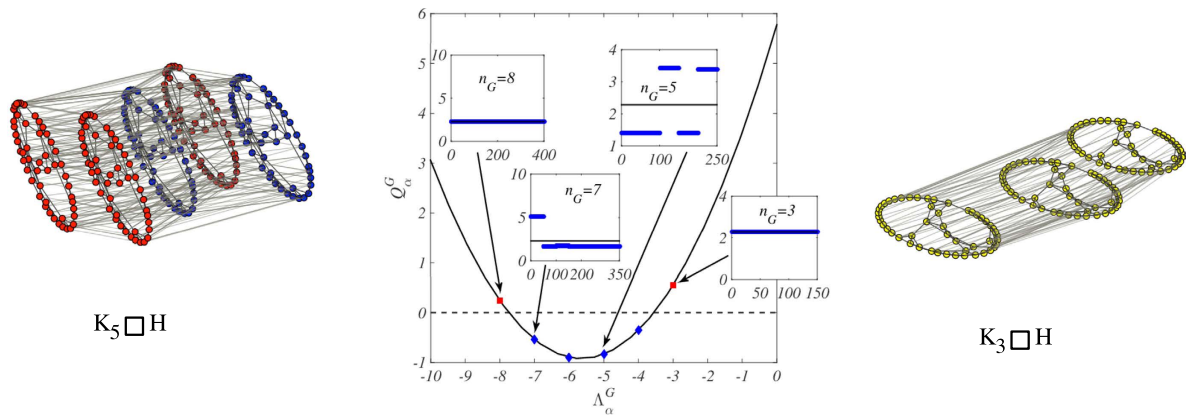


Figure 5. Turing patterns for the Mimura-Murray model on a multiplex $G \square H$, with G complete network. Left panel: Turing Patterns (for the species u) in the multiplex $K_5 \square H$ ($n_G = 5$), where H is the network obtained by using the Watts-Strogatz algorithm²³ with $n_H = 50$, $p_H = 0.04$ and average degree $\langle k_H \rangle = 4$. Blue nodes correspond to nodes where the asymptotic concentration of species u is larger than the homogeneous values $\hat{u} \sim 2.28$ ($u_i(t_\infty) - \hat{u} > \hat{u}/10$); red nodes correspond to nodes where the asymptotic concentration of species u is lower than the homogeneous values $\hat{u} \sim 2.28$ ($u_i(t_\infty) - \hat{u} < -\hat{u}/10$). To help the reader only 40% of links among different layers have been drawn. Notice that the patterns results in a segregation between activator rich - activator poor layers. This is an interesting self-organized stationary solution of the reaction diffusion model, that we will describe in details elsewhere. Middle panel: Q_α^G is plotted versus Λ_α^G . n_G denotes the nodes of the complete network G . Once again, H is a Watts-Strogatz²³ network composed by $n_H = 50$ nodes, with a probability to rewire a link equal to $p_H = 0.04$ and average degree $\langle k_H \rangle = 4$. Turing patterns can develop if and only if $Q_\alpha^G > 0$ for some Λ_α^G . For the complete network $\Lambda_1^G = 0$ and $\Lambda_\alpha^G = -n_G$ for $\alpha > 1$ with multiplicity $n_G - 1$. Hence, Q_α^G is negative if and only if $q_- < -n_G < q_+$. For our choice of the parameters (see below), one finds $q_- \sim 7.74$ and $q_+ \sim 3.55$. Turing patterns can hence develop on G , and thus on the multiplex $G \square H$, if and only if $-7 \leq n_G \leq -4$. This is confirmed by inspection of the annexed insets, where the asymptotic concentration of species u is reported against an integer which runs over the nodes, for different choices of n_G . This result follows a numerical integration of the relevant reaction-diffusion equations. The horizontal solid lines represent the unperturbed homogeneous fixed point. Here, the diffusion coefficients are $D_u^G = 0.1$, $D_v^G = 2.1$, $D_u^H = 1.12$ and $D_v^H = 2.6$. The initial condition is set as explained in the caption of Fig. 2. Right panel: absence of Turing Patterns (for the species u) in the multiplex $K_3 \square H$ ($n_G = 3$), where H is again a network obtained using the Watts-Strogatz algorithm with $n_H = 50$, $p_H = 0.04$ and average degree $\langle k_H \rangle = 4$. Yellow nodes correspond to nodes where the asymptotic concentration of species u is equal to the homogeneous values, $u_i(t_\infty) = \hat{u} \sim 2.28$, for all i . To help the reader only 40% of links among different layers have been drawn.

beginning on the simplified setting where the Cartesian product involves two distinct networks, but the analysis, as well as the conclusions of our study, apply to a more general setting where several networks can be combined together to give a multidimensional Cartesian Product. The dispersion relation which ultimately determines the onset of the instability is now function of two independent set of discrete wavelengths, the eigenvalues of the Laplacian operators constructed from the two networks that combine in the Cartesian structure. As a consequence, the process of patterns formation for a reaction-diffusion system on Cartesian support can be rationalized via an integrated approach which moves from the analysis of the instability conditions on each of the graphs taken independently. In particular, we could prove that patterns can invade the Cartesian network, if they are supported on one of the graphs that compose its structure. Multiplex networks can be also obtained as a special limiting case and the domain of instability delimited by compact relations. When a generic network is assembled with a complete graph to yield a degenerate multi-dimensional complex lattice, the onset of the instability can be controlled by the number of nodes of the complete sub-structure. Our findings have been corroborated by direct numerical integration of the reaction-diffusion equations, assuming the Mimura-Murray kinetics as a representative model.

References

- Murray, J. D. in *Mathematical Biology II: Spatial Models and Biomedical Applications*, 3rd edn, Ch. 2, 71–140 (Springer, 2011).
- Zhabotinsky, A. M., Dolnik, M. & Epstein, I. R. Pattern Formation Arising from Wave Instability in a Simple Reaction-Diffusion System. *J. Chem. Phys.* **103**, 10306–10314 (1995).
- Turing, A. M. The Chemical Basis of Morphogenesis. *Phil. Trans. R. Soc. London B* **237**, 37–72 (1952).
- Othmer, H. G. & Scriven, L. E. Instability and dynamic pattern in cellular networks. *J. Theor. Biol.* **32**, 507–537 (1971).

5. Nakao, H. & Mikhailov, A. S. Turing patterns in network-organized activator-inhibitor systems. *Nature Physics* **6** 544–551; doi: 10.1038/NPHYS1651 (2010)
6. Asllani, M., Busiello, D. M., Carletti, T., Fanelli, D. & Planchon, G. Turing patterns in multiplex networks. *Phys. Rev. E* **90**, 042814-1–042814-5; doi: 10.1103/PhysRevE.90.042814 (2014).
7. Asllani, M., Challenger, J. D., Saverio Pavone, F., Sacconi, L. & Fanelli, D. Topology-driven instabilities: the theory of pattern formation on directed networks. *Nature Communications* **5**, 4517-1–4517-9; doi: 10.1038/ncomms5517 (2014).
8. Mucha, P. J. *et al.* Community structure in time-dependent, multiscale, and multiplex networks. *Science* **328**, 876–878; doi: 10.1126/science.1184819 (2010).
9. Gomez-Gardenes, J., Reinares, L., Arenas, A. & Floria, L. M. Evolution of cooperation in multiplex networks. *Sci. Rep.* **2**, 620-1–620-6; doi: 10.1038/srep00620 (2012).
10. Bianconi, G. Statistical mechanics of multiplex networks: Entropy and overlap. *Phys. Rev. E* **87**, 062806-1–062806-15; doi: 10.1103/PhysRevE.87.062806 (2013).
11. Morris, R. G. & Barthelemy, M. Transport on coupled spatial networks. *Phys. Rev. Lett.* **109**, 128703-1–128703-4; doi: 10.1103/PhysRevLett.109.128703 (2012).
12. Nicosia, V., Bianconi, G., Latora, V. & Barthelemy, M. Growing multiplex networks. *Phys. Rev. Lett.* **111**, 058701-1–058701-5; doi: 10.1103/PhysRevLett.111.058701 (2013).
13. Kivela, M. *et al.* Multilayer networks. *J. Complex Networks* **2**, 203–271; doi: 10.1093/comnet/cnu016 (2014).
14. Boccaletti, S. *et al.* The structure and dynamics of multilayer networks. *Phys. Rep.* **544**, 1–122; doi: 10.1016/j.physrep.2014.07.001 (2014).
15. Massaro, E. & Bagnoli, F. Epidemic spreading and risk perception in multiplex networks: A self-organized percolation method. *Phys. Rev. E* **90**, 052817-1–052817-8; doi: 10.1103/PhysRevE.90.052817 (2014).
16. Vizing, V. G. The Cartesian Product of Graphs. *Vychisl. Sistemy* **9**, 30–43 (1963).
17. Chapman, A., Nabi-Abdolyousefi, M. & Mesbahi, M. On the Controllability and Observability of Cartesian Product Networks. *Proceedings of the 5th IEEE Conference on Decision and Control*. Maui, Hawaii, USA (2012).
18. Atay, F. M. & Bıykoğlu, T. Graph operations and synchronisation of complex networks. *Phys. Rev. E* **72**, 016217-1–016217-7; doi: 10.1103/PhysRevE.72.016217 (2005).
19. Imrich, W. & Klavzar, S. in *Product Graph* 1st edn, pages 27 and following (Wiley-Interscience, 2000).
20. Asllani, M., Di Patti, F. & Fanelli, D. Stochastic Turing patterns on a network. *Phys. Rev. E* **86**, 046105-1–046105-6; doi: 10.1103/PhysRevE.86.046105 (2012).
21. Asllani, M., Biancalani, T., Fanelli, D. & McKane, A. J. The linear noise approximation for reaction-diffusion systems on networks. *Eur. Phys. J. B* **86**, 1–10; doi: 10.1140/epjb/e2013-40570-8 (2013).
22. Mimura, M. & Murray, J. D. Diffusive prey-predator model which exhibits patchiness. *J. Theor. Biol.* **75**, 249–262 (1978).
23. Watts, D. J. & Strogatz, S. H., Collective dynamics of small-world networks. *Nature* **393**, 440–442 (1998).

Acknowledgments

The work of T.C. presents research results of the Belgian Network DYSCO (Dynamical Systems, Control, and Optimization), funded by the Interuniversity Attraction Poles Programme, initiated by the Belgian State, Science Policy Office.

Author Contributions

M.A., D.M.B., T.C., D.F. and G.P. designed and carried out the study. T.C. and D.F. wrote the main manuscript text. D.M.B., G.P. and T.C. prepared figs 2 and 4. T.C. prepared figs 1, 3 and 5. All authors reviewed and approved the manuscript.

Additional Information

Competing financial interests: The authors declare no competing financial interests.

How to cite this article: Asllani, M. *et al.* Turing instabilities on Cartesian product networks. *Sci. Rep.* **5**, 12927; doi: 10.1038/srep12927 (2015).



This work is licensed under a Creative Commons Attribution 4.0 International License. The images or other third party material in this article are included in the article's Creative Commons license, unless indicated otherwise in the credit line; if the material is not included under the Creative Commons license, users will need to obtain permission from the license holder to reproduce the material. To view a copy of this license, visit <http://creativecommons.org/licenses/by/4.0/>